

Active Damping of Structures with Guy Cables

A. Preumont* and Y. Achkire†
Free University of Brussels, 1050 Brussels, Belgium

A strategy is presented for active damping of structures with guy cables. The active member consists of a piezoelectric actuator collocated with a force sensor. The control algorithm consists of an integral force feedback; it has guaranteed stability, including at the parametric resonance. The results are confirmed by an experiment. Also described is an efficient modeling technique for cable structures; simple and powerful results are established, which permit prediction of the closed-loop poles with a root locus technique. This technique is demonstrated on a guyed truss.

I. Introduction

THE current design of the space station is largely based on trusses, but it is quite likely that the future large space structures (LSS) will use large trusses connected by tension cables, to increase their global stiffness, in a way similar to that used to stiffen the airplanes in the early days of aeronautics. This concept of tension truss structure has already been used for large mesh antennas (a 10-m deployable mesh antenna was flown by the Russians in 1979); it has the advantages of being deployable and easily reconfigurable by changing the static tension in the cables and of lending itself naturally to shape control.^{1,2}

The active damping of LSS has long been recognized as a major issue for various reasons such as the interaction of the flexible modes with the attitude control system, the pointing requirements of various instruments mounted on the station, or simply preservation of the microgravity environment. The active damping of truss structures has received considerable attention for the past 10 years or so, and effective solutions have been proposed^{3,4}; active struts including piezoelectric actuators have been developed, and control laws with guaranteed stability have been tested successfully.⁵

The active damping of cable structures is more difficult because cables and strings behave in a nonlinear manner and are prone to parametric excitation when the frequency of the supporting structure is close to twice the natural frequency of the cable. Chen⁶ showed that the vibration of a string can be controlled by a positive use of the parametric excitation resulting from the longitudinal motion of the support at a frequency equal to twice the frequency of the transverse vibration of the string (stiffness control).

The damping of cable structures has also become a major issue in civil engineering because the ever-increasing span of the cable-stayed bridges⁷ makes them more sensitive to wind and traffic induced vibrations as well as to flutter instability. The distinctive feature here is the presence of some sag in the vertical plane, resulting from the gravity loads (typical value of the sag to length ratio is 0.5%). The active damping of cable-stayed bridges with an active tendon has been investigated by Warnitchai et al.⁸ and Susumpow and Fujino⁹; the various strategies investigated for damping the main structure and the in-plane and out-of-plane vibration of the cable are represented in Fig. 1. They demonstrated that the vertical global mode of the bridge can be damped with a linear feedback of the girder velocity on the active tendon displacement (Fig. 1a); the in-plane (vertical) local cable vibration can be controlled very efficiently by sag induced forces (Fig. 1b). Sag induced forces do not affect the out-of-plane local vibration of the cable, but the stiffness control discussed earlier can be applied (Fig. 1c); however, experimental results¹⁰ have shown that an instability can occur when the cable structure interaction is large, especially when the struc-

ture's natural frequency is close to twice that of the cable, causing the time-varying tension to resonate with the structure. Note that the following strategies use a noncollocated pair of sensor and actuator and are prone to spillover.¹¹ In a recent paper,¹² the present authors have proposed an alternative control strategy with guaranteed stability; it will be reviewed in Sec. II. Section III will present some experimental results. Section IV describes briefly an efficient modeling technique for cable structures; it is applied to a truss with guy cables in Sec. V. Section VI presents an approximate linear theory leading to a root locus technique for the closed-loop poles prediction.

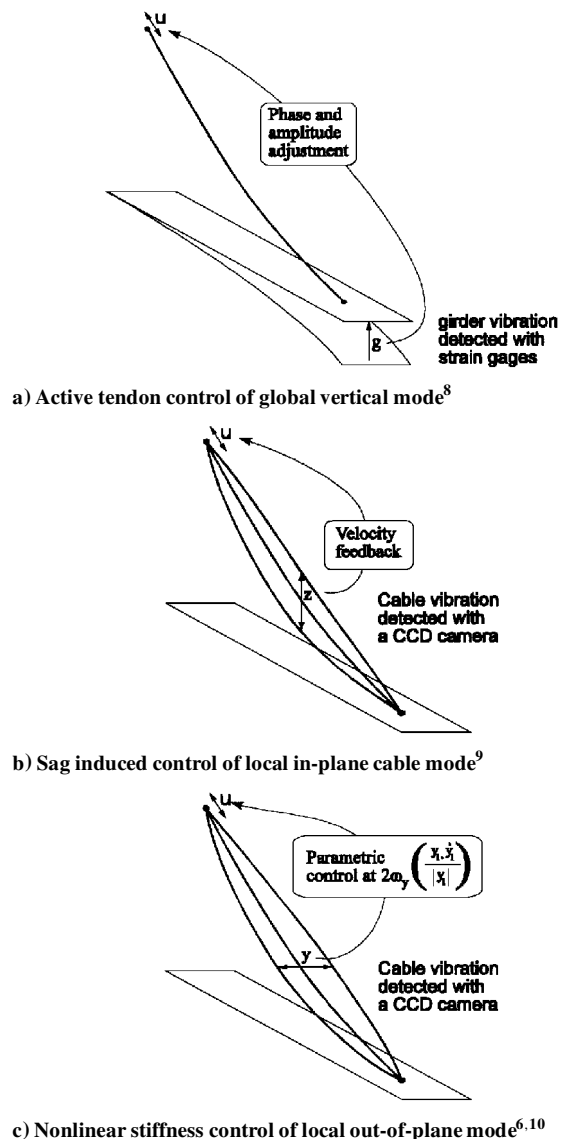


Fig. 1 Existing control strategies.

Received April 29, 1996; revision received Nov. 8, 1996; accepted for publication Nov. 8, 1996. Copyright © 1996 by the American Institute of Aeronautics and Astronautics, Inc. All rights reserved.

*Professor, Active Structures Laboratory, Department of Mechanical Engineering and Robotics, 50 av. F. D. Roosevelt. Member AIAA.

†Ph.D. Fellow (Fonds pour la formation à la Recherche dans l'Industrie et dans l'Agriculture), Active Structures Laboratory, 50 av. F. D. Roosevelt.

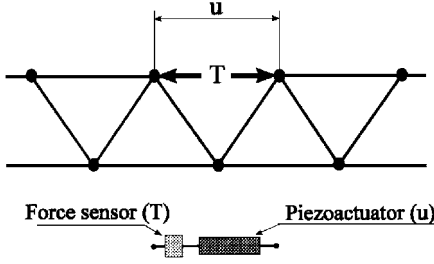


Fig. 2 Force feedback.

The present discussion is not directly relevant to space tethers because the level of strain considered here is at least one order of magnitude larger. Moreover, the tether systems are tension controlled,¹³ whereas the cable structure systems considered here are displacement controlled (with very small stroke).

II. Control Strategy

It is widely accepted that active damping of linear structures is much simplified if one uses collocated actuator and sensor pairs¹⁴; for such configurations, a wide class of controllers with guaranteed stability can be developed.^{15,16}

For nonlinear structures, the use of collocated actuator-sensor pairs is still quite attractive because there exist control schemes that are guaranteed to be energy absorbing, in the sense that the energy flows from the structure into the control system, at least if we assume perfect actuator and sensor dynamics; such control laws are asymptotically stable. One of them is the well-known direct velocity feedback; less known is the dual situation where the actuator controls the relative position u of two points inside the structure (e.g., piezoelectric linear actuator) and the collocated sensor output is the force T in the active member (Fig. 2).

The power flow from the control system is

$$W = -T\dot{u} \quad (1)$$

and it is readily verified that the positive integral force feedback

$$u = g \int T \, dt \Rightarrow W = -gT^2 \quad (g > 0) \quad (2)$$

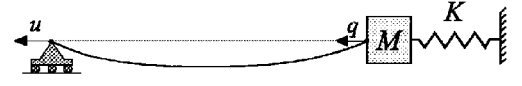


Fig. 3 Cable structure system.

produces an energy absorbing control if we assume perfect actuator and sensor dynamics. This control law was already applied to the active damping of a truss structure in Ref. 5, but it is quite remarkable that it is also applicable to nonlinear structures. All of the states that are controllable and observable will be asymptotically stable for any value of g (infinite gain margin). To appreciate what this means, consider the governing equations of the mass-spring system attached to a cable^{8,12} (Fig. 3); the governing equations are given by Eqs. (3–6), where z_n and y_n refer to the modal amplitudes of the in-plane (vertical) and out-of-plane modes, respectively; u is the axial motion of the support and q that of the structure. The analytical form of the coefficients can be found in Ref. 8; the physical meaning of the various terms is indicated in the equations. The fact that the in-plane natural frequency ω_{zn} is larger than the corresponding out-of-plane frequency ω_{yn} is due to the sag. We observe that the additional term in the equation of the spring-mass system is exactly the tension in the cable. In the cable equations, notice that the active sag induced force appears only in Eq. (4) governing the in-plane motion and only for the symmetric modes, because $\alpha_n = 0$ if n is even. On the contrary, the active stiffness variation affects all the modes. In Eq. (6), h_u is the static stiffness of the cable; we see that all the cable modes affect the tension in the cable with the quadratic term, corresponding to cable stretching, but only the in-plane modes of odd number have a linear influence on T , because $h_{1n} = 0$ if n is even.

From the foregoing equations, we can anticipate that the control algorithm will be effective for the global mode of the structure and the local in-plane symmetric modes of the cables, which are linearly controllable and observable. For the in-plane nonsymmetric modes and the out-of-plane modes of the cables, which are observable only through their quadratic contribution to the cable stretching, and controllable only through the active stiffness variation, the control system is likely to be effective only for large amplitudes; its effectiveness will gradually reduce to zero as the vibration amplitude decreases. These observations have been confirmed by the following experiment:

Out-of-plane:

$$m_{yn}(\ddot{y}_n + 2\xi_{yn}\omega_{yn}\dot{y}_n + \omega_{yn}^2 y_n) - \sum_k v_{nk} y_n (y_k^2 + z_k^2) + \sum_k 2\beta_{nk} y_n z_k - R_n q y_n + R_n u y_n = F_{yn} \quad (3)$$

In-plane:

$$m_{zn}(\ddot{z}_n + 2\xi_{zn}\omega_{zn}\dot{z}_n + \omega_{zn}^2 z_n) + \sum_k v_{nk} z_n (y_k^2 + z_k^2) + \sum_k 2\beta_{nk} z_n z_k - R_n q z_n + R_n u z_n + \sum_k \beta_{kn} (y_k^2 + z_k^2) + \alpha_n \dot{q} - \alpha_n \ddot{u} = F_{zn} \quad (4)$$

Structure:

$$M(\ddot{q} + 2\xi_q\omega_q\dot{q} + \omega_q^2 q) + h_u q - h_u u - \sum_n h_{2n} (y_n^2 + z_n^2) - \sum_n h_{1n} z_n = F_q \quad (5)$$

Cable tension:

$$T = \underbrace{h_u u}_{\text{Feedthrough}} - h_u q + \sum_n h_{2n} (y_n^2 + z_n^2) + \sum_n h_{1n} z_n \quad (6)$$

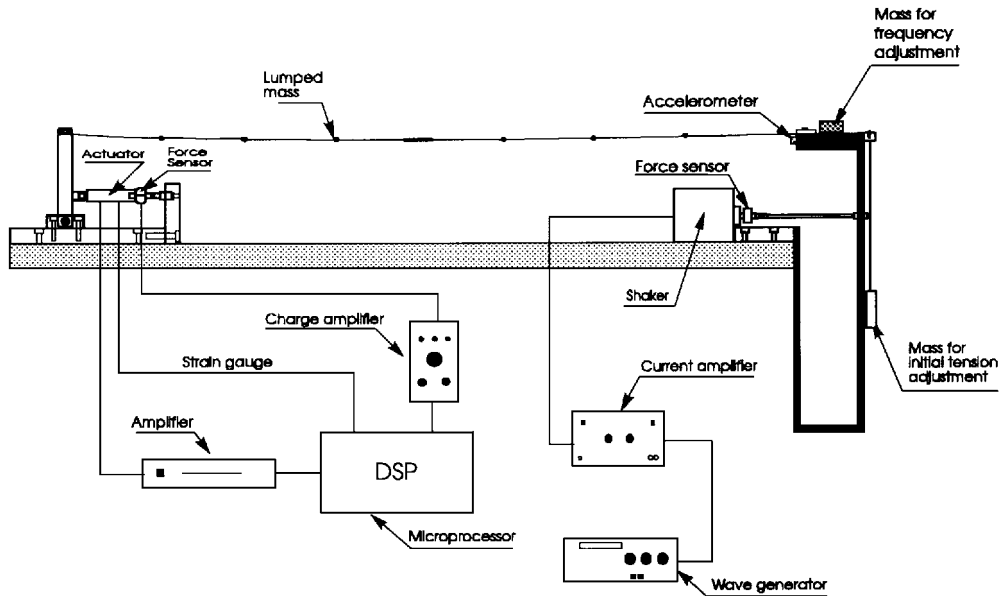


Fig. 4 Cable-structure system experimental setup.

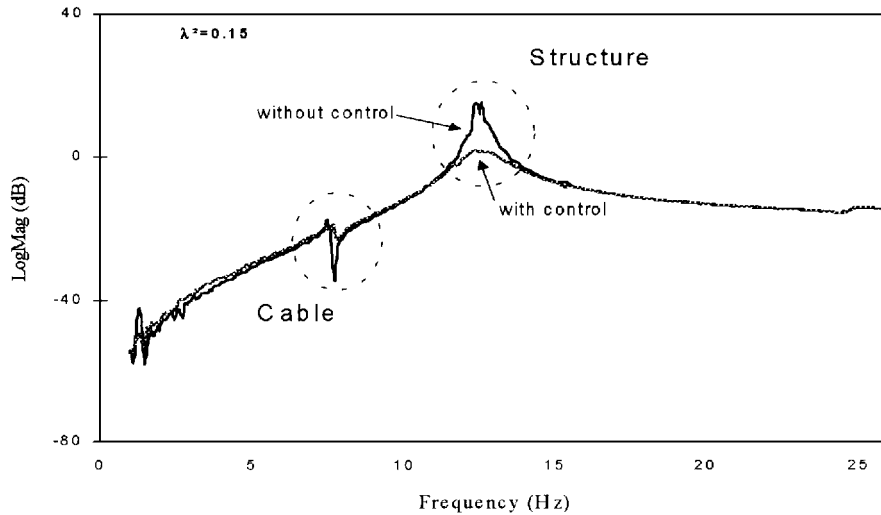


Fig. 5 Experimental frequency response function between the shaker and the accelerometer, with and without control.

III. Experiment

Figure 4 shows the test structure adopted to represent the ideal situation of Fig. 3; the cable is a 2-m-long stainless steel wire of 0.196-mm² cross section provided with additional lumped masses at regular intervals to achieve a sag-to-span ratio of 0.5% when the first in-plane natural frequency is $f_{z1} = 5.7$ Hz. The active tendon is materialized by a piezoelectric linear actuator acting on the support point with a lever arm to amplify the actuator displacement by a factor 3.4; this produces a maximum axial displacement of 150 μ m for the moving support.

A piezoelectric force sensor is colinear with the actuator; because of the high-pass behavior of this type of sensor, it measures only the dynamic component of the tension in the cable. The controller is implemented digitally on a digital signal processor board. The spring-mass system has an adjustable mass to tune its natural frequency; a shaker and an accelerometer are attached to it to evaluate the performances of the control system. In addition to that, a non-contact laser measurement system was developed to measure the cable displacement.¹⁷

Experiments have been conducted with the cable alone and the cable structure system; they are described in more detail in Ref. 12. The effect of the control system on the structure is displayed in Figs. 5 and 6 when $f_{\text{cable}} = 8$ Hz, $f_{\text{structure}} = 12.6$ Hz, and the sag-to-span ratio $d/l = 0.21\%$. Figure 5 shows the frequency response

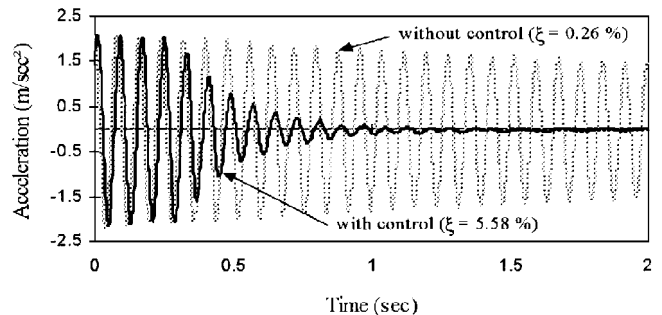


Fig. 6 Free response of the structure, with and without control.

function between the shaker and the accelerometer mounted on the structure; the free response of the structure from nonzero initial conditions is shown in Fig. 6; we see that the control system brings a substantial amount of damping in the system. As far as the cable modes are concerned, the out-of-plane modes and the antisymmetric in-plane modes are not affected by the control system, except for large amplitudes where the cable stretching becomes significant; the amount of active damping brought into the symmetric in-plane modes depends very much on the sag-to-span ratio. The control system behaves nicely even at the parametric resonance, when

the natural frequency of the structure is exactly twice that of the cable.

IV. Modeling of Cable Structures

Consider the cable structure of Fig. 7, consisting of a linear structure (here a truss) with a number of nodes interconnected with cables. As an alternative to a general nonlinear finite element approach, which would be extremely time consuming, especially for control system design purposes, we have developed a dedicated software that combines a finite element model of the linear structure with an analytical model of the cables in modal coordinates. This model is an extension of that of the cable connected to the spring-mass system of Eqs. (3–6); the model of each cable is written in a local coordinate system as indicated in Fig. 7; the local x axis is taken along the chord line, whereas the z axis is in the gravity plane (it is arbitrary in a zero-gravity environment).

The governing equations are given in Eqs. (7–10); they result from Lagrange's equations, using the modal amplitudes as generalized coordinates and a nonlinear strain-displacement relationship; their development, as well as the analytical expressions of the various constants, will be given in a separate report.¹⁸ The tension in the cable is identical to Eq. (6); it can be decomposed into a quasistatic contribution T_q^i from the axial motion of the supports and a dynamic one resulting from the cable stretching and the sag. If we substitute Eq. (7) into Eq. (8), it becomes identical to Eq. (3), except for the additional terms due to the seismic excitation produced by the transverse acceleration of the supports, \ddot{v}_a , \ddot{v}_b , \ddot{w}_a , and \ddot{w}_b , which was ignored in Eq. (3). As compared with Eq. (8), Eq. (9) has two additional terms due to the sag: the sag induced stiffness and the sag induced inertia. The sag induced stiffness $\Lambda_n^i T_d^i$ has a linear and a quadratic contribution; the linear one is responsible for the increase of the natural frequency of the cable in the vertical plane [$\omega_{zn} > \omega_n$ in Eq. (4)]. The sag induced inertia $-\alpha_n^i (\ddot{u}_b^i - \ddot{u}_a^i)$ is the inertia force induced by the axial acceleration of the supports.

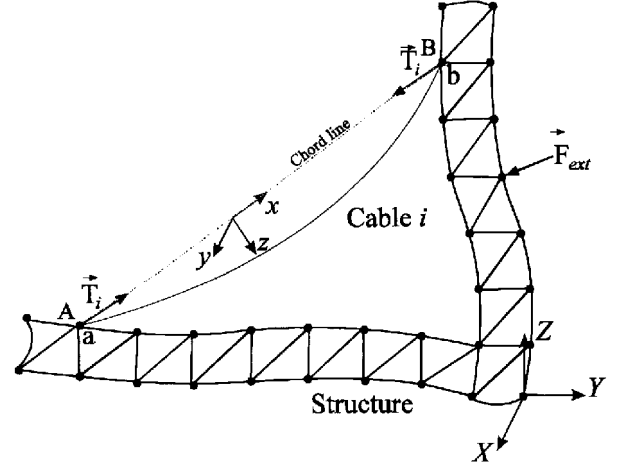


Fig. 7 Cable structure model.

The structure equation (10) is written in the global system of coordinates; the left-hand side is obtained from a standard finite element code; the sum in the right-hand side represents the forces applied to the structure by the cables; it consists of the axial loads of the cable tension and the reaction forces due to the transverse vibration of the cable. The rotation matrix P^i transforms the cable loads from the local to the global coordinate systems. The structure equation is further transformed into modal coordinates to reduce the number of degrees of freedom.

In Eqs. (7–10), an active tendon control placed at one end of a cable (say a in Fig. 7) contributes to the quasistatic tension T_q^i for $-h_u^i u_a^i$ and also to the inertia forces $-\alpha_n^i \ddot{u}_a^i$ that affect only the in-plane modes of the cable. The term T_q^i appears in all of the equations

Cable i

Cable tension:

$$T^i = T_q^i + T_d^i = \underbrace{h_u^i (u_b^i - u_a^i)}_{T_q^i : \text{Quasistatic tension}} + \underbrace{\sum_n h_{1n}^i z_n^i}_{\text{Cable sag}} + \underbrace{\sum_n h_{2n}^i (y_n^{i2} + z_n^{i2})}_{\text{Stretching due to cable vibration}} \quad (7)$$

T_d^i : Dynamic tension

Out-of-plane equation (mode n):

$$m_{zn} (\ddot{y}_n^i + 2\xi_{yn} \omega_n \dot{y}_n^i + \omega_n^2 y_n^i) + \underbrace{S_n^i (T_q^i + T_d^i)}_{\text{Stiffness variation}} y_n^i + \underbrace{\Gamma_n^i [\ddot{v}_a^i + (-1)^{n+1} \ddot{v}_b^i]}_{\text{Seismic excitation due to support transverse motion}} = F_{yn}^i \quad (8)$$

In-plane equation (mode n):

$$m_{zn} (\ddot{z}_n^i + 2\xi_{zn} \omega_n \dot{z}_n^i + \omega_n^2 z_n^i) + \underbrace{S_n^i (T_q^i + T_d^i)}_{\text{Stiffness variation}} z_n^i + \underbrace{\Gamma_n^i [\ddot{w}_a^i + (-1)^{n+1} \ddot{w}_b^i]}_{\text{Seismic excitation due to support transverse motion}} + \underbrace{\Lambda_n^i T_d^i}_{\text{Sag stiffness}} - \underbrace{\alpha_n^i (\ddot{u}_b^i - \ddot{u}_a^i)}_{\text{Inertia force due to support axial movement}} = F_{zn}^i \quad (9)$$

Structure

$$M\ddot{x} + C\dot{x} + Kx = \sum_i^{nc} P^i \left\{ \underbrace{T_q^i + T_d^i}_{\text{Cable tension}} + \underbrace{\sum_n G_{yn}^i \ddot{y}_n^i + G_{zn}^i \ddot{z}_n^i}_{\text{Reaction forces due to the transverse motion of the cable}} \right\} + F_{\text{ext}} \quad (10)$$

and $h_u^i(u_b^i - u_a^i)$ is, in fact, the main contributor to the control of the structure, whereas $-\alpha_n^i(\ddot{u}_b^i - \ddot{u}_a^i)$ is the main source of control for the in-plane modes of the cables.

Equations (7–10) must be supplemented by the control algorithm; assuming that the active tendons are located at extremity a of the cables, the control law for active damping is simply

$$u_a^i = g \int_0^t T_d^i(\tau) d\tau \quad (11)$$

where T_d^i is the dynamic contribution of the tension in the cable (it is the only one that is sensed by a piezoelectric force sensor because of the high-pass behavior of the charge amplifier).

To avoid numerical saturation, Eq. (11) is slightly changed to introduce a forgetting factor, and to account for the finite stroke of the actuator, it is combined with a saturation unit. Once the equations

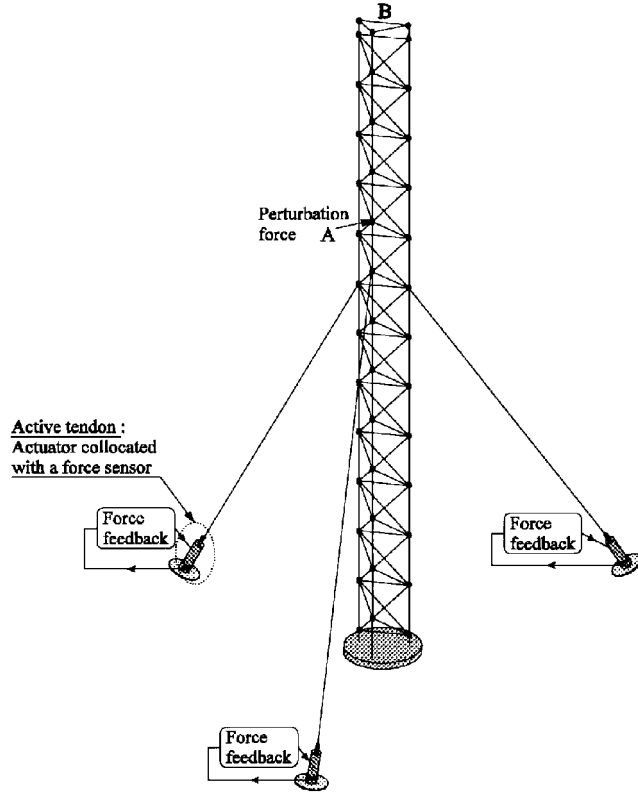


Fig. 8 Guyed truss.

have been formulated, it is a simple matter to integrate the response of the closed-loop system for any external perturbation and arbitrary initial conditions.

V. Truss with Guy Cables

As an example of application, consider the 12 bay truss with three guy cables of Fig. 8; the truss alone was already considered in Ref. 5, where its active damping was achieved with two active struts located in the first bay starting from the bottom. Here, we investigate the possibility to control the system with three guy cables of 1-mm in diameter attached to the truss as indicated on the figure and provided with an active tendon at their base, at a distance of 1 m from the truss; we assume no gravity, so that the cables behave like strings. Without control, the net effect of the cables is to stiffen the truss, raising its natural frequencies; the control system affects both the natural frequencies and the damping of the modes. Figure 9 shows the evolution of the resonant peaks of the frequency response between a point force applied along the truss (A in Fig. 8) and an accelerometer placed at the top, when the gain g of the control law (11) is changed (the same gain is used for every active tendon). These results have been obtained by solving numerically Eqs. (7–10), taking into account the physical data of the actuators, including their finite stroke.

We observe that, when the gain increases, the two resonant peaks drop very quickly, then move horizontally toward the lower frequency, and then start to rise again at high gains, to become identical to the resonant peaks of the truss without guy cables. This behavior is the consequence of the well-known fact that when we increase the gain, the closed-loop poles start from the open-loop poles and move toward the open-loop zeros. Because the zeros are, by definition, the frequencies of the input (the voltage at the piezo) where the output (the cable tension) vanishes, the tension in the cables becomes equal to zero and the guyed truss behaves like the free one.

VI. Approximate Linear Theory

In a situation like the one described in the previous section, the cables are extremely light and behave essentially like strings. If we assume that the interaction between the structure and the active cables is restricted to the tension in the cables and if one neglects the cable dynamics, the governing equation is

$$M\ddot{x} + Kx = -BT \quad (12)$$

where K refers to the structure without guy cables, T is the vector of tension in the guy cables, and B is the influence matrix. If we neglect the cable dynamics, the tension in the cables is given by

$$T = K_c(B^T x - \delta) \quad (13)$$

where K_c is the stiffness matrix of the cables, $K_c = \text{diag}(h_u)$, $B^T x$ are the relative displacements of the extremities of the cables, and

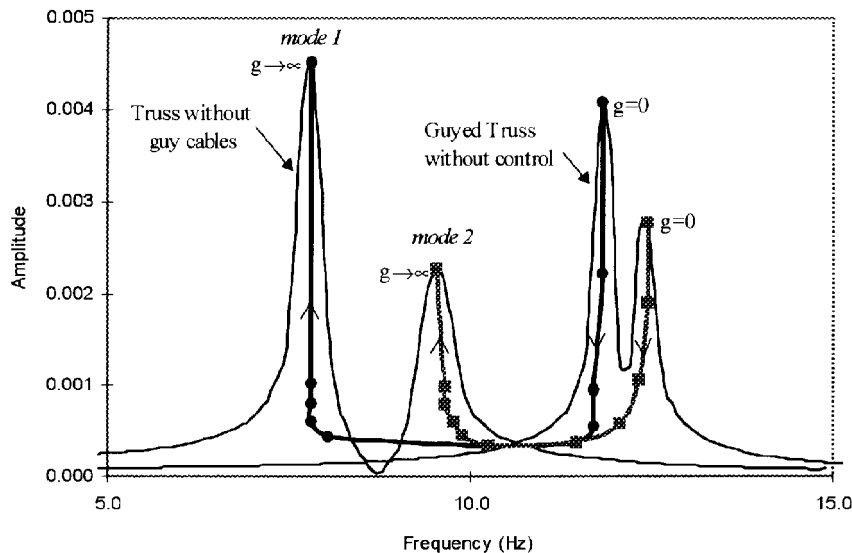


Fig. 9 Evolution of the resonant peaks of the frequency response between A and B in Fig. 8 when the control gain g is changed.

δ are the active displacements of the tendons. Combining Eqs. (12) and (13), we get

$$M\ddot{x} + (K + BK_c B^T)x = BK_c \delta \quad (14)$$

which indicates that $K + BK_c B^T$ is the stiffness matrix of the structure with guy cables. We assume that all the guy cables have the same control law with the same gain,

$$\delta = (g/sh_u)T \quad (15)$$

Combining with Eq. (13), we have

$$\delta = [g/(s + g)]B^T x \quad (16)$$

Substituting in Eq. (14), we obtain the closed-loop equation

$$[Ms^2 + (K + BK_c B^T) - [g/(g + s)]BK_c B^T]x = 0 \quad (17)$$

From this equation, it is readily observed that as $g \rightarrow \infty$, the dynamics of the closed-loop system converge toward that of the structure without cables, as we observed in the numerical experiment of the previous section.

Let us project Eq. (17) on the normal modes $x = \Phi z$ of the structure with cables, assumed normalized according to $\Phi^T M \Phi = I$. If we denote $\Omega^2 = \Phi^T (K + BK_c B^T) \Phi$, Eq. (17) becomes

$$[s^2 + \Omega^2 - [g/(g + s)]\Phi^T BK_c B^T \Phi]z = 0 \quad (18)$$

To derive a simple and powerful result about the way each mode evolves with g , let us assume that the mode shapes are little changed by the active cables, so that we can write

$$\begin{aligned} \Omega^2 &= \Phi^T (K + BK_c B^T) \Phi \\ &= \Phi^T K \Phi + \Phi^T BK_c B^T \Phi = \omega^2 + v^2 \end{aligned} \quad (19)$$

where the two matrices ω^2 and v^2 are also diagonal. This hypothesis is identical to that made to derive Jacobi's eigenvalue perturbation formula.¹⁵ In this case, $\omega^2 = \Phi^T K \Phi$ contains the square of the natural frequencies of the structure without the active cables.

Substituting Eq. (19) into Eq. (18), we obtain a set of decoupled equations; the characteristic equation for mode i is

$$\begin{aligned} s^2 + \Omega_i^2 - [g/(s + g)](\Omega_i^2 - \omega_i^2) &= 0 \quad \text{or} \\ s(s^2 + \Omega_i^2) + g(s^2 + \omega_i^2) &= 0 \end{aligned} \quad (20)$$

This equation shows that the poles go from $\pm j\Omega_i$ for $g = 0$ to $\pm j\omega_i$ for $g \rightarrow \infty$ (as we have already seen) and that, in between, they follow the root locus corresponding to the open-loop transfer function

$$G(s) = g \frac{s^2 + \omega_i^2}{s(s^2 + \Omega_i^2)} \quad (21)$$

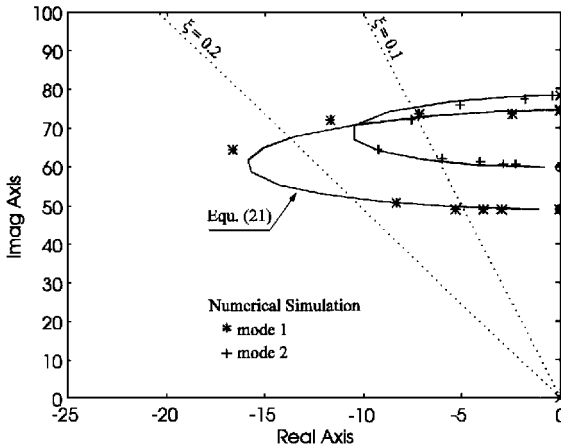


Fig. 10 Comparison of the root locus with the numerical simulation.

where the poles and the zeros correspond to the natural frequencies of the structure with and without the active cables, respectively. Figure 10 compares the prediction of the foregoing linear theory with the numerical experiment performed with the full model already reported in Fig. 9; we see that the agreement is quite good.

According to the foregoing discussion, if a cable structure has a set of active cables that are such that the mode shapes of the structure, with and without the active cables, are not significantly different, every closed-loop pole corresponding to the decentralized integral force feedback follows the root locus defined by Eq. (21), where Ω_i is the natural frequency of the structure with the active cables and ω_i that of the structure without the active cables (but including the passive ones if any).

The maximum value of the modal damping ξ_i can be evaluated with a perturbation method: if we substitute $s = \Omega_i[-\xi_i + j(1 + \delta_i)]$ in Eq. (20) and neglect the second-order terms in ξ_i and δ_i , we find easily

$$\xi_i = \frac{g(\Omega_i^2 - \omega_i^2)}{2\Omega_i(\Omega_i^2 + g^2)} \quad (22)$$

$$\delta_i = -(g\xi_i/\Omega_i) \quad (23)$$

From Eq. (22), the maximum modal damping is achieved for $g^* = \Omega_i$; we find

$$\xi_i^{\max} = \frac{(\Omega_i^2 - \omega_i^2)}{4\Omega_i^2} \quad (24)$$

If we assume that $(\Omega_i + \omega_i) \approx 2\Omega_i$, this result can be further simplified into

$$\xi_i^{\max} \approx \frac{(\Omega_i - \omega_i)}{2\Omega_i} \quad (25)$$

Thus, the maximum modal damping is controlled by the relative spacing of the natural frequencies with and without the active cables.

This result provides a simple rationale for selecting the number, the size, and the location of the active cables in the first step of the design process.

VII. Conclusion

The first part of this paper presents a strategy for active damping of cable structures, using an active tendon collocated with a force sensor. The guaranteed stability has been confirmed by experimental results, even at the parametric resonance.

The second part of the paper describes an efficient modeling technique for cable structures; it is applied to a truss with guy cables, and the numerical results are compared with linear predictions. Simple and powerful results are established, which allow one to predict the closed-loop poles with a root locus technique.

References

- Mitsugi, J., Yasaka, T., and Miura, K., "Shape Control of the Tension Truss Antenna," *AIAA Journal*, Vol. 28, No. 2, 1990, pp. 316-322.
- Miura, K., and Miyazaki, Y., "Concept of the Tension Truss Antenna," *AIAA Journal*, Vol. 28, No. 6, 1990, pp. 1098-1104.
- Fanson, J. L., Blackwood, C. H., and Chu, C. C., "Active Member Control of a Precision Structure," *Proceedings of the AIAA/ASME/ASCE/AHS 30th Structures, Structural Dynamics, and Materials Conference*, AIAA, Washington, DC, 1989, pp. 1480-1494.
- Chen, G. S., Lurie, B. J., and Wada, B. K., "Experimental Studies of Adaptive Structure for Precision Performance," *Proceedings of the AIAA/ASME/ASCE/AHS 30th Structures, Structural Dynamics, and Materials Conference*, AIAA, Washington, DC, 1989, pp. 1462-1472.
- Preumont, A., Dufour, J.-P., and Malékian, C., "Active Damping by a Local Force Feedback with Piezoelectric Actuators," *Journal of Guidance, Control, and Dynamics*, Vol. 15, No. 2, 1992, pp. 390-395.
- Chen, J.-C., "Response of Large Space Structures with Stiffness Control," *Journal of Spacecraft and Rockets*, Vol. 21, No. 5, 1984, pp. 463-467.
- Yamaguchi, H., "Modal Damping of Suspended Cables," *Proceedings of Damping '89* (West Palm Beach, FL), Wright Aeronautical Labs., WRDC-TR-89-3116, 1989, pp. GBC1-13.
- Warnitchai, P., Fujino, Y., Pacheco, B. M., and Agret, R., "An Experimental Study on Active Tendon Control of Cable-Stayed Bridges," *Earthquake Engineering and Structural Dynamics*, Vol. 22, 1993, pp. 93-111.

⁹Susumpow, T., and Fujino, Y., "An Experimental Study on Active Control of Planar Cable Vibration by Axial Support Motion," *Earthquake Engineering and Structural Dynamics*, Vol. 23, 1994, pp. 1283–1297.

¹⁰Fujino, Y., Warnitchai, P., and Pacheco, B. M., "Active Stiffness Control of Cable Vibration," *Journal of Applied Mechanics*, Vol. 60, No. 4, 1993, pp. 948–953.

¹¹Balas, M. J., "Active Control of Flexible Systems," *Journal of Optimization Theory and Applications*, Vol. 25, No. 3, 1978, pp. 415–436.

¹²Achkire, Y., and Preumont, A., "Active Tendon Control of Cable-Stayed Bridges," *Earthquake Engineering and Structural Dynamics*, Vol. 25, No. 6, 1996, pp. 585–597.

¹³Rupp, C. C., "A Tether Tension Control Law for Tethered Subsattellites Deployed Along the Local Vertical," NASA TMX-64963, Sept. 1975.

¹⁴Cannon, R. H., and Rosenthal, D. E., "Experiment in Control of Flexible

Structures with Noncollocated Sensors and Actuators," *Journal of Guidance, Control, and Dynamics*, Vol. 7, 1984, pp. 546–553.

¹⁵Aubrun, J. N., "Theory of the Control of Structures by Low-Authority Controllers," *Journal of Guidance and Control*, Vol. 3, No. 5, 1980, pp. 444–451.

¹⁶Benhabib, R. J., Iwens, R. P., and Jackson, R. L., "Stability of Large Space Structures Control Systems Using Positivity Concepts," *Journal of Guidance and Control*, Vol. 4, 1981, pp. 487–494.

¹⁷Achkire, Y., and Preumont, A., "Optical Measurement of Cable and String Vibration," *Proceedings of the 2nd International Conference on Vibration Measurements by Laser Techniques* (Ancona, Italy), SPIE, Vol. 2868, 1996, pp. 540–549.

¹⁸Achkire, Y., "Active Tendon Control of Cable-Stayed Bridges," Ph.D. Dissertation, Active Structures Lab., Dept. of Mechanical Engineering, Université Libre de Bruxelles, Belgium (in preparation).